Tutor/s
Dr. Jordi Guilera Sala
Departament d'Enginyeria Química i Química Analítica

Dra. Elena Martin Morales
Institut de Recerca en Energia de Catalunya (IREC)

Grau de Química

Treball Final de Grau

Preparation of methanol reforming catalysts by Atomic Layer Deposition (ALD).
Preparació de catalitzadors per a la reformació de metanol mitjançant Deposició de Capes Atòmiques (ALD).

Carles Graell Hernández
(06/2025)

Universitat de Barcelona
B:KC Barcelona Knowledge Campus
Campus d'Excel·lència Internacional

Aquesta obra esta subjecta a la llicència de:
Reconeixement–NoComercial-SenseObraDerivada

http://creativecommons.org/licenses/by-nc-nd/3.0/es/

Vull agrair a l'Elena Martín (supervisora de l'IREC) tot el suport, l'acompanyament al llarg d'aquest projecte i el fet d'haver-me descobert la recerca amb rigor i il·lusió. També vull donar les gràcies al meu supervisor de la UB, en Jordi Guilera, per les seves idees i consells.

A la meva família i als meus amics, gràcies per l'escolta i l'empara rebudes durant aquest temps.

També vull donar les gràcies a totes aquelles persones de l'IREC que directament o indirecta han contribuït a fer possible aquest estudi.

Ha sigut un plaer per mi poder formar part d'aquest projecte, endinsar-me durant aquests mesos en el món de la recerca i poder observar de primera mà els reptes que planteja la transició energètica.

REPORT

IDENTIFICATION AND REFLECTION ON THE SUSTAINABLE DEVELOPMENT GOALS (SDG)

The synthesis and performance evaluation of $CuO/ZnO/Al_2O_3$ (CZA) catalysts for methanol steam reforming (MSR) directly contributes to several Sustainable Development Goals (SDGs), particularly those focused on clean energy, industry innovation, and climate action. By exploring ways to minimize zinc oxide content while enhancing catalyst activity and stability through Atomic Layer Deposition (ALD), this study addresses critical challenges in producing clean hydrogen, a key energy vector for the transition towards a sustainable future.

Methanol is a promising hydrogen carrier due to its high hydrogen content, ease of storage, and potential for sustainable production from biomass or carbon dioxide. The ability to efficiently convert methanol into hydrogen using optimized CZA catalysts supports SDG 7, which aims to ensure access to affordable, reliable, sustainable, and modern energy for all. The improved catalytic performance, especially in terms of higher methanol conversion and lower CO selectivity observed in ALD-prepared catalysts, reflects advancements that can enhance hydrogen production efficiency and reduce harmful emissions, making this approach environmentally advantageous.

Moreover, the application of ALD as a synthesis technique represents a significant innovation aligning with SDG 9, which promotes resilient infrastructure, inclusive and sustainable industrialization, and innovation. ALD's atomic-level precision in catalyst design allows for better control of material usage and catalyst properties, which can lead to more durable and effective catalysts while reducing waste and material consumption.

From a climate action perspective, linked to SDG 13, this research supports the reduction of gas emissions through cleaner hydrogen production pathways. By limiting CO formation and improving catalyst longevity, the study contributes to mitigating environmental impacts associated with hydrogen production and use.

Looking forward, the continuation and scaling of this project could have far-reaching societal benefits. Advancements in catalyst technology for MSR could facilitate broader adoption of hydrogen as a clean fuel in transportation and industry, reducing reliance on fossil fuels and promoting energy security. Additionally, the integration of ALD techniques in catalyst manufacturing may stimulate economic growth by creating new opportunities in advanced manufacturing and green technologies, aligning with the broader goals of sustainable development.

In summary, this study not only advances fundamental knowledge in catalyst science but also aligns with key SDGs by promoting clean energy innovation, sustainable industrial processes, and climate change mitigation. Its contributions exemplify how targeted research can support global efforts to build a more sustainable future.

CONTENTS

1. SUMMARY

Methanol Steam Reforming (MSR) is of particular interest for fuel cell applications and integrated hydrogen production systems, both as a transportation fuel and for industrial applications, given methanol's favorable characteristics as a hydrogen carrier. $CuO/ZnO/Al_2O_3$ (CZA) catalysts for MSR have been widely employed due to their high activity, selectivity, and stability under reaction conditions.

This study investigates the synthesis and performance of CZA catalysts for MSR, with a focus on minimizing ZnO content and evaluating Atomic Layer Deposition (ALD) as an alternative to conventional preparation methods. Catalysts with fixed CuO loading and varying ZnO content were prepared by wet impregnation and ALD, and were characterized using XRD, N_2 physisorption, and H_2-TPR. Catalytic activity was assessed in MSR reactions between 250–350 °C.

Results revealed that a low ZnO loading (1 wt%) provided favorable textural properties, while the highest methanol conversion was achieved with 10 wt% ZnO. ALD-prepared catalysts demonstrated improved stability and activity at moderate temperatures, along with lower CO selectivity, highlighting the potential of ALD for enhancing catalyst performance.

Keywords: hydrogen carrier, Methanol Steam Reforming, CZA, ALD.

2. RESUM

El reformat de metanol amb vapor d'aigua (MSR) és d'especial interès per a aplicacions en piles de combustible i sistemes integrats de producció d'hidrogen, tant com a combustible per a la mobilitat com per a aplicacions industrials, donades les característiques favorables del metanol com a portador d'hidrogen. Els catalitzadors de $CuO/ZnO/Al_2O_3$ (CZA) per a MSR són àmpliament emprats gràcies a la seva alta activitat, selectivitat i estabilitat en les condicions de reacció.

Aquest estudi investiga la síntesi i el rendiment dels catalitzadors CZA per a MSR, fent especial èmfasi en la minimització del contingut de ZnO i l'avaluació de la deposició per capes atòmiques (ALD) com a alternativa als mètodes convencionals de síntesi com la impregnació humida. Per assolir aquest objectiu, s'han sintetitzat catalitzadors amb composició fixa de CuO i contingut variable de ZnO mitjançant impregnació humida i ALD, i s'han caracteritzat mitjançant difracció de raigs X (XRD), fisisorció de N_2 i reducció amb H_2 a temperatura programada (H_2-TPR). L'activitat catalítica s'ha avaluat en reaccions de MSR entre 250 i 350 °C.

Els resultats obtinguts revelen que una baixa composició de ZnO (1 % en pes) proporciona major porositat, mentre que la conversió més alta de metanol s'ha aconseguit amb un 10 % en pes de ZnO. Els catalitzadors preparats per ALD han demostrat una millor estabilitat i activitat a temperatures moderades, i una menor selectivitat a CO, fet que destaca el potencial de l'ALD per millorar el rendiment del catalitzador.

Paraules clau: Portador d'hidrogen, reformat de metanol amb vapor d'aigua, CZA, ALD.

3. INTRODUCTION

3.1 METHANOL AS A HYDROGEN CARRIER

Methanol stands out as a highly suitable hydrogen carrier due to its high hydrogen storage capacity, reaching up to 99 kg per cubic meter[1]. Additionally, it is cost-effective, readily accessible, and can be sustainably produced from biomass through gasification, a thermochemical process that converts organic materials into synthesis gas (a mixture of CO and H_2), which is then catalytically converted into methanol[2] or through the hydrogenation of carbon dioxide, where H_2 is greenly produced and CO_2 is fixed from the atmosphere[3].

Beyond its high hydrogen content and ease of production, methanol offers high volumetric energy, low sulfur content, ease of handling (it remains líquid under ambient conditions). Altogether, these properties position methanol as a promising vector in hydrogen energy research and applications.

3.2 MSR FUNDAMENTALS AND CONDITIONS

Methanol Steam Reforming (MSR) is of particular interest for fuel cell applications and integrated hydrogen production systems as a transportation fuel or for industrial applications, given methanol's favorable characteristics as a hydrogen carrier[4]. MSR is a widely studied process for hydrogen production due to its relatively low operating temperatures, favorable hydrogen-to-carbon ratio, and enhanced conversion efficiency, which altogether lead to high hydrogen yields[5].

In this endothermic reaction, methanol (CH_3OH) reacts with water vapor (H_2O) over a heterogeneous catalyst to yield hydrogen (H_2) and carbon dioxide (CO_2), according to the overall stoichiometry:

$$CH_3OH + H_2O \rightarrow CO_2 + 3H_2, \Delta H^\circ = +49.4 \text{ kJ mol}^{-1} \quad \text{Eq [1]}^6$$

The reaction typically proceeds at temperatures between 250–300 °C and atmospheric pressure[7]. An important parameter to consider is the methanol-to-water ratio, as it has been demonstrated that a ratio greater than 1 contributes to increased methanol conversion and reduced CO formation. However, increasing the ratio beyond 2 leads to a decrease in energy efficiency, making the optimal range lie between a ratio of 1 and 2[8]. It is also essential to control undesired side reactions in order to avoid CO formation, wich can deactivate the catalyst[1], such as:

$$CH_3OH \rightarrow CO + 2H_2 \quad \text{Eq [2]}^1$$

Maintaining the reaction temperature below 300 °C effectively suppresses the formation of carbon monoxide[9] as shown in Figure 1.

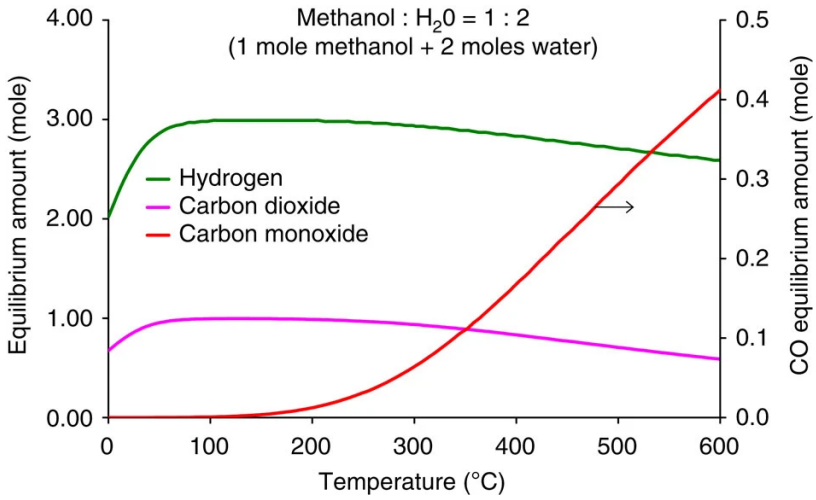

Figure 1: Thermodynamic equilibrium product compositions[10]

3.3 CATALYSTS FOR MSR

The design of MSR catalysts that achieve efficient methanol conversion, high hydrogen production, minimal carbon monoxide formation, and long-term operational stability remains a key and complex objective. Achieving long-term stability is particularly challenging due to catalyst deactivation, primarily caused by active phase sintering and carbon monoxide-induced poisoning[11]. Among the various catalysts investigated, copper-based systems (notably $Cu/ZnO/Al_2O_3$) and palladium-based materials (such as Pd/ZnO) have emerged as the most prominent due to their high activity, selectivity, and stability under reaction conditions[1].

According to the literature, $CuO/ZnO/Al_2O_3$ (CZA) catalysts commonly employed for methanol steam reforming typically consist of approximately 65 wt% copper oxide (CuO), 25 wt% zinc oxide (ZnO), and 10 wt% alumina (Al_2O_3) [12], prepared by various methods such as coprecipitation, impregnation, and sol–gel techniques [13]. In addition to the conventional $CuO/ZnO/Al_2O_3$ system, a wide range of catalyst formulations have been investigated for MSR, reflecting the intense research interest in optimizing hydrogen production. These include Cu–Mn oxides, Cu/Zn/Zr/Al mixed oxides, Cu-based catalysts supported on ZrO_2 or Al_2O_3[13].

Some examples of CZA catalysts employed for MSR are show in Table 1:

Catalyst	Al_2O_3 [wt%]	ZnO[wt%]	CuO[wt%]	.Method	Reference.
1	11	23	66	–	[12]
2	20	30	50	Sol-gel	[14]
3	7	63	30	Assisted combustion	[15]
4	80	5	15	Impregnation	[16]
5	1	30	69	Sol-gel	[17]
6	15	16	69	Precipitation	[18]
7	19	31	50	Impregnation	[19]

Table 1: CZA catalyst composicions employed for MSR

The ternary $Cu/ZnO/Al_2O_3$ (CZA) catalyst is widely employed in methanol steam reforming due to its unique combination of activity, selectivity, and stability. In this system, alumina (Al_2O_3) serves as the support and contributes significantly by enhancing the mechanical strength of the catalyst and providing resistance to sintering, while also facilitating copper reduction, as shown by temperature-programmed reduction (TPR) [20]. Additionally, alumina exhibits a promotional effect by increasing the dispersion of copper species and influencing the reducibility of ZnO, further contributing to the overall catalytic performance.

Zinc oxide plays a complementary role by interacting with copper nanoparticles through strong metal–support interactions (SMSI), which suppress sintering and help maintain catalytic performance [21] as shown in Figure 2

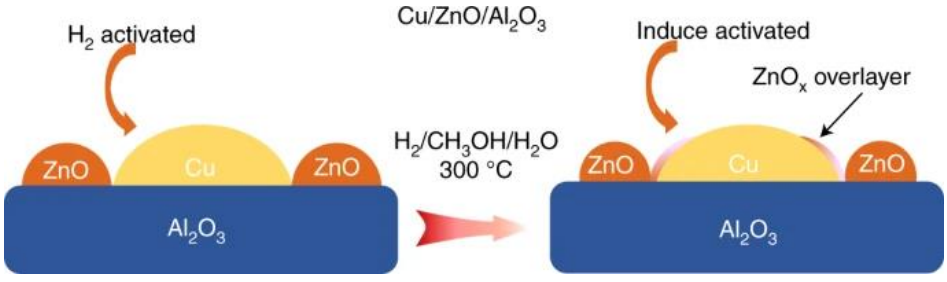

Figure 2: Zinc oxide by interacting with copper nanoparticles through strong metal–support interactions (SMSI)[21]

The active phase of the catalyst is primarily attributed to metallic copper (Cu^0), which provides the key sites for methanol activation. However, an excessive amount of copper can accelerate catalyst deactivation due to sintering and agglomeration of the metal particles[22]. The inclusion of ZnO helps mitigate this issue by stabilizing copper species and promoting the formation of Cu–ZnO interfacial sites. Cu–ZnOx interfacial sites are responsible for the improved activity. Maximizing the number of these accessible Cu–ZnOx interfacial regions leads to superior catalytic performance. Therefore, precise control over the ZnOx overlayer thickness is essential to ensure adequate exposure of these active sites. The Cu–ZnOx interface is characterized by the coexistence of Cu^+ and

partially oxidized Zn species (Zn^δ^+, where $0 < \delta < 2$) [21]. This synergy between Cu, ZnO, and Al_2O_3 results in a robust and efficient catalyst, making CZA the preferred system for MSR.

The use of CZA catalysts in MSR requires optimization of their composition and structure, given their dependency on large amounts of zinc and copper. Controlling the interface may be key to generating new active sites and reducing material usage. This underscores the value of employing advanced deposition techniques, such as Atomic Layer Deposition (ALD).

3.4 Atomic Layer Deposition for Catalysts

The layer-by-layer nature of Atomic Layer Deposition (ALD) allows for exceptional precision in constructing materials with carefully defined structural and compositional features, an advantage of great relevance for catalyst design. Nowadays, ALD is used in industrial applications such as semiconductor fabrication in microelectronics and solid oxide fuel cells (SOFCs) in the energy industry[23]. Among its key capabilities is the formation of porous surface coatings that can encapsulate metal particles and limit their tendency to sinter. Additionally, the robustness of ALD-derived coatings under high-temperature conditions has been documented in several studies, highlighting the suitability of this technique for catalytic systems operating under severe environments. Altogether, these characteristics make ALD a powerful and versatile tool for the development of next-generation catalysts[23].

Understanding the operational mechanism of Atomic Layer Deposition is essential when considering its application in the synthesis of advanced CZA catalysts. A typical ALD cycle, shown in Figure 3, is composed of four sequential and self-limiting steps, each of which contributes to the atomic precision that characterizes this technique. Initially, a metal volatile precursor is introduced into the reaction chamber, where it chemisorbs onto the available surface sites of the support material. This adsorption is inherently self-limiting, as the reaction halts once all reactive sites are occupied. The chamber is then purged with an inert gas to remove any unreacted precursor and gaseous byproducts. Subsequently, a second reactant—commonly an oxidizing or reducing agent—is introduced to react with the adsorbed species, eliminating residual ligands and regenerating surface functionalities required for subsequent cycles. A final purge step ensures the complete evacuation of reaction byproducts and unreacted gas molecules. By repeating this sequence, it becomes possible to construct highly controlled thin films or dispersed phases with unparalleled uniformity, making ALD a valuable tool in the precise design of heterogeneous catalysts[23]. These attributes position ALD as a promising approach for advancing the structural and functional performance of CZA catalysts in methanol steam reforming applications.

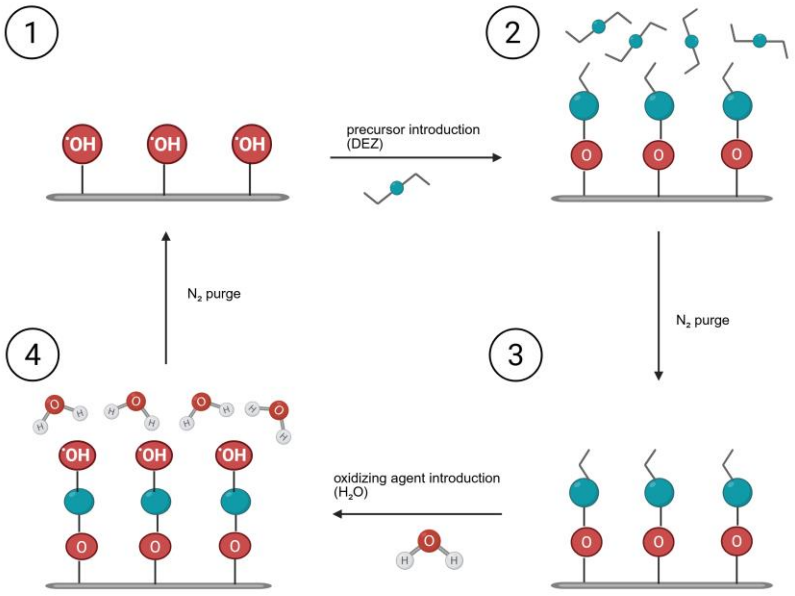

Figure 3: An ALD process consists of several cycles, each made up of the following exposure steps: (1) purge, (2) precursor vapour pulse, (3) purge and (4) reactant gas pulse.

3.5 ZnO ALD-based catalyst

Zinc oxide thin films deposited by (ALD) are gaining increasing attention due to their excellent optical transparency, high growth uniformity, and suitability for low-temperature processing. These features make ZnO highly attractive for a wide range of applications, including piezoelectric devices, transparent conductive electrodes, solar cells, gas sensors, LEDs, and thin-film transistors[24]. Among the various zinc precursors used, diethylzinc (DEZ) is the most common, thanks to its high volatility and reactivity[24]. However, its pyrophoric nature has encouraged the development of safer alternatives such as $Zn(DMP)_2$[25], dimethylzinc (DMZ)[26], and the diethylzinc-dimethyl ethylamine (DEZDMEA) adduct, which offer improved stability under moderate temperatures [24]. ALD of ZnO is typically carried out between room temperature and 200 °C on substrates like silicon, SiO_2/Si [27], and alumina nanoparticles[28], demonstrating versatility across both materials and device platforms.

3.6 Context and scope

This study is part of the Road2H2 project, which aims to develop a methanol and ethanol reformer for hydrogen production that can address the challenges associated with hydrogen transport and distribution. The project involves Viver Clean Tech, a company focused on developing innovative technologies to provide sustainable energy solutions, and IREC, which will lead the research, development, and implementation of the microcatalysts.

The application of ALD on CZA micropellets addresses the need for enhanced catalyst stability and uniformity in industrial reactors, where large-scale operation imposes strict demands on long-term performance under dynamic process conditions.

4. OBJECTIVES

The main objective of this study is to optimize and minimize the amount of ZnO in CuO/ZnO/Al_2O_3 (CZA) catalysts for the Methanol Steam Reforming (MSR) reaction, a key process for efficient hydrogen production.. This research aims to provide deeper insight into the influence of synthesis methodology and composition on catalyst performance.

To achieve this overall goal, the following specific studies will be carried out:

· Synthesize a series of catalysts with a fixed CuO loading of 10 wt.% and varying ZnO contents ranging from 1 to 10 wt.% using conventional methods such as wet impregnation and innovative methods such as Atomic Layer Deposition (ALD).

· Characterize the structural, textural and redox properties of the synthesized catalysts using X-ray diffraction (XRD), nitrogen physisorption (N_2 adsorption–desorption), and hydrogen temperature-programmed reduction (H_2-TPR).

· Evaluate the catalytic activity of catalysts synthesized via Atomic Layer Deposition (ALD) with those prepared through conventional wet impregnation methods, in order to assess the effect of the synthesis technique on catalytic properties.

· Identification of the optimal synthesis conditions and compositional parameters required for the development of catalysts with enhanced activity, improved selectivity, and greater stability under Methanol Steam Reforming operating conditions.

5. EXPERIMENTAL SECTION

5.1 CATALYST PREPARATION

Table 2 presents the synthesized catalysts, including the support used, the composition of the components, and the synthesis method employed. Figure 4 shows the synthesized catalysts.

Catalyst ID	Support	ZnO[wt%]	CuO[wt%]	Method
$CuO–Al_2O_3$	Al_2O_3	0	10	Wet impregnation
$1ZnO–CuO–Al_2O_3$	$CuO–Al_2O_3$	1	10	Wet impregnation
$10ZnO–CuO–Al_2O_3$	$CuO–Al_2O_3$	10	10	Wet impregnation
$ALDZnO–CuO–Al_2O_3$	$CuO–Al_2O_3$	<1	10	ALD
$1ZnO–Al_2O_3$ (reference)	Al_2O_3	1	0	Wet impregnation
$10ZnO–Al_2O_3$ (reference)	Al_2O_3	10	0	Wet impregnation
$ALDZnO–Al_2O_3$ (reference)	Al_2O_3	<1	0	ALD

Table 2: Oxide compositions of the synthesized catalysts and reference samples.

Figure 4: a) $CuO–Al_2O_3$ b) $1ZnO–CuO–Al_2O_3$, c) $10ZnO–CuO–Al_2O$ d) $ALDZnO–CuO–Al_2O_3$ e)$1ZnO–Al_2O_3$ f) $10ZnO–Al_2O_3$ g) $ALDZnO–Al_2O_3$ catalysts.

A **$CuO–Al_2O_3$** catalyst was synthesized by dissolving 6.81 g of $Cu(NO_3)_2{\cdot}2.5H_2O$ in 50 mL of water, followed by the addition of 20.16 g of 0.5 mm diameter mesoporous alumina Accu-Spheres Saint-Gobain Norpro. The mixture was stirred for 45 min at room temperature and atmospheric pressure, then the solvent was removed at 75 °C and 100 mbar under constant agitation until complete solvent removal. The resulting solid was dried at 105 °C for 10 h and subsequently calcined at 450 °C for 4 h.

Based on the previously prepared $CuO–Al_2O_3$ catalyst, two ZnO-promoted samples were synthesized by wet impregnation. For the **$1ZnO–CuO–Al_2O_3$** catalyst, 0.07 g of $Zn(NO_3)_2{\cdot}6H_2O$ was dissolved in 5 mL of water and impregnated onto 1.91 g of the Cu-based support. For the **$10ZnO–CuO–Al_2O_3$** catalyst, 0.86 g of $Zn(NO_3)_2{\cdot}6H_2O$ was dissolved in 5 mL of water and added to 1.85 g of the same support. Both mixtures were stirred for 2 h at room temperature, dried at 75 °C and 100 mbar under constant stirring, and subjected to thermal treatment at 105 °C for 10 h and 450 °C for 4h.

A ZnO-promoted sample was synthesized from the $CuO–Al_2O_3$ catalyst using Atomic Layer Deposition (ALD) Figure 6 and 7. For the **$ALDZnO–CuO–Al_2O_3$** catalyst, 0.75 g of $CuO–Al_2O_3$ was weighed. Diethylzinc (DEZ) was used as ZnO precursor and water (H_2O) as the oxidizing agent, with nitrogen (N_2) as the inert gas. The process was conducted at 200 °C for 100 cycles.

Each cycle involved a 0.1-second water pulse, a nitrogen purge (40 seconds, 150 sccm), a 0.1-second DEZ pulse, and a second identical purge. A 60-second stop-flow period is always applied between the precursor pulse and the nitrogen purge. For a better understanding of the reactor purging system, Figure 5 shows the relationship between time, the actions carried out, and the source line pressure.

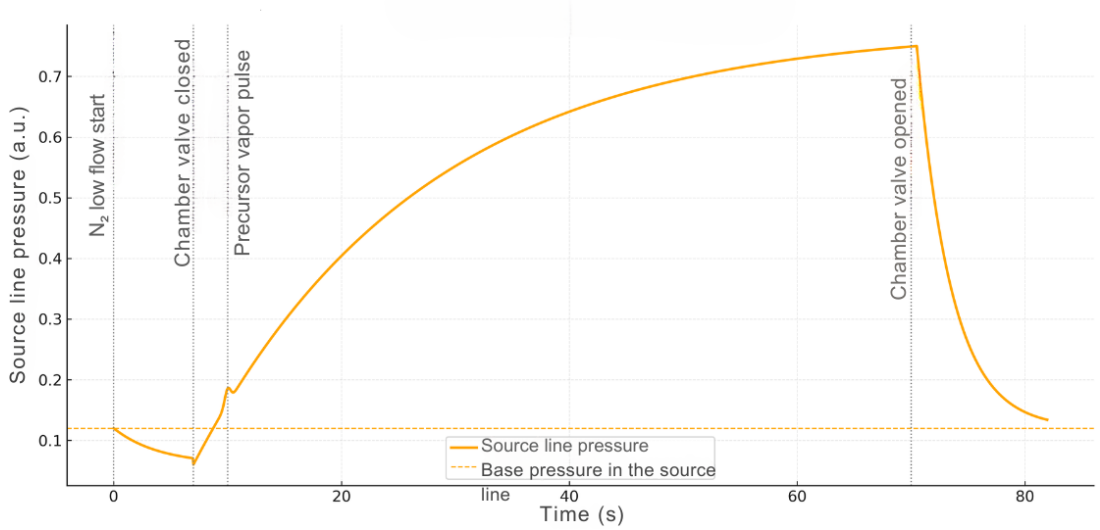

Figure 5: The graph illustrates the pressure variation before the purging of the gas line, along with the actions that induce these changes.

Two reference materials, containing only ZnO and Al_2O_3, were prepared by the same impregnation method. For the **1ZnO–Al_2O_3** reference, 0.39 g of $Zn(NO_3)_2{\cdot}6H_2O$ were dissolved in 25 mL of water and impregnated onto 10.03 g of alumina. For the **10ZnO–Al_2O_3** catalyst, 4.10 g of $Zn(NO_3)_2{\cdot}6H_2O$ was dissolved in 25 mL of water and added to 10.16 g of alumina. Both mixtures were stirred for 2 h at ambient conditions, dried at 75 °C and 100 mbar under constant agitation, and thermally treated at 105 °C for 10 h and 450 °C for 4 h.

A third reference was synthesized by depositing ZnO onto Al_2O_3 pellets via Atomic Layer Deposition (ALD) Figure 6 and 7. For the **ALDZnO–Al_2O_3** reference, 0.38 g of Alumina Accu-Spheres was weighed. Diethylzinc (DEZ) was used as the zinc precursor and water (H_2O) the oxidizing agent, with nitrogen (N_2) serving as the inert carrier gas. The deposition process was carried out at 200°C over 100 cycles. The ALD parameters applied were identical to those used for the synthesis of ZnO-promoted Cu-based catalysts.

In addition to the synthesized catalysts, commercial catalyst HyProGen 251 was used to compare their performance and properties.

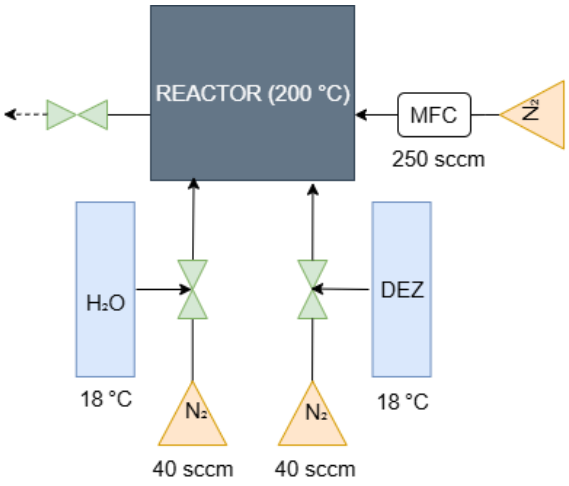

Figure 6: ALD reactor scheme

Figure 7: Picosun ALD reactor

5.2 CHARACTERIZATION

5.2.1 XRD

The determination of the crystalline structure and phase composition of the analysed materials was carried out using X-ray diffraction (XRD). Sample preparation involved grinding into fine powder and mixed with isopropanol to form a slurry. The mixture was drop-cast onto a silicon substrate and dried under ambient conditions. X-ray diffraction (XRD) patterns were collected within the 2Θ range 20-80° in a Bruker type XRD D8 Advance A25 diffractometer using a Cu Kα radiation (λ = 1.5406 Å), a voltage of 40 kV, a current of 40 mA and a step size of 0.02° (with 2 s duration at each step). The average crystal sizes of CuO were estimated using the Scherrer's equation at 2θ = 35.5° for (-111) [3]:

$$D = (K \cdot \lambda)/(\beta \cdot \cos\Theta) \quad [3]$$

The values of X-ray wavelength and Scherrer constant are respectively λ = 1.5406 Å and K = 0.9.

5.2.2 Nitrogen physisorption

The determination of surface area and pore size distribution for the analysed materials was carried out using nitrogen physisorption. This analysis was performed with the aid of a Micromeritics FlowPrep 060 and a Micromeritics TriStar II system, both operating in conjunction with dedicated software capable of regulating temperature and continuously tracking gas volume and system pressure.

Before proceeding with the measurements, the samples were subjected to a degassing under N2 flow. Initially, they were heated to 90 °C for 1 hour, then heated at 250 °C for 5 hours. Once complete degassing had been achieved, the isotherm was recorded at liquid N2 temperature: vacuum was applied, and an accurately measured volume of nitrogen gas was introduced while monitoring the pressure variations throughout the process. When the maximum relative pressure was reached, vacuum was reapplied. By applying appropriate mathematical models, the BET surface area (SABET), pore volume, and pore size distribution were calculated.

5.2.3 H_2-TPR

The determination of the oxidation states of the oxides in the analyzed materials was carried out using Temperature Programmed Reduction (H_2-TPR). These analyses were conducted with an Autochem 2890 (Micromeritics) using a 50 NmL/min flow of H_2 (12% H_2 in Ar). This technique measures the temperatures at which the samples are reduced in the presence of hydrogen.

5.3 CATALYTIC REACTION

Prior to each activity test, the evaluated catalysts were subjected to an in-situ reduction process at 300 °C for 1 h under a total flow of 100 mL min^{-1} (10 mL min^{-1} H_2 and 90 mL min^{-1} N_2). After reduction, the system was cooled to 50 °C maintaining a 15mL min^{-1} N_2 before introducing the reactants. For each experiment, 0.15 g of catalyst was thoroughly mixed with 1.5 g of silicon carbide (SiC).

Steam-reforming experiments were performed between 250 °C and 350 °C in 25 °C steps. A liquid feed consisting of methanol and water molar H_2O/CH_3OH ratio of 1.3. was injected by a synringe pump (0.02 mL min^{-1}) to evaporate the liquid, and the steam was mixed in the reactor with 30 mL min^{-1} of N_2 wich acted as carrier gas.

The outlet stream first passed through a 0 °C cold trap to condense unreacted methanol and water. The dry product gas was then analyzed online with an 490 micro-gas chromatograph equipped with a thermal conductivity detector. Methanol conversion ($X_{m\ e}OH$), selectivities to CO (S_{CO}) and the weight hour space velocity ($WHSV_{CH_3OH}$) were calculated according to Eqs. [4–5]

$$X_{CH_3OH} = \frac{CO\ (outlet) + CO_2\ (outlet) + CH_4\ (outlet)}{CH_3OH\ (inlet)} \quad [4]$$

$$S_{CO}(\%) = \frac{nCO}{nCO + nCO_2 + nCH_4} \quad [5]$$

6. RESULTS AND DISCUSSION

6.1 STRUCTURAL PROPERTIES OF THE SAMPLES

6.1.1 X-ray Diffraction (XRD) Analysis

CZA catalyst

The XRD of the synthesized catalysts (**$CuO–Al_2O_3$, ALDZnO–$CuO–Al_2O_3$, 1 $ZnO–CuO–Al_2O_3$, 10 ZnO– $CuO–Al_2O_3$** and **Commercial,**) are presented in (Fig 8). The typical diffraction peaks for CuO at 2Θ= 32.5°(-1 1 0), 35.5°(-1 1 1), 38.7° (1 1 1), 48.7° (-2 0 2), 53.5° (0 2 0), 58.3° (2 0 2) and 61.5° (-1 1 3) and ZnO hexagonal wurtzite structure 2Θ°=31.8° (1 0 0), 34.4° (0 0 2), 36.2° (1 0 1), 47.5° (1 0 2) and 56.6° (1 1 0) have been identified and indicated in Figure 8.

The XRD patterns of all CZA catalysts display diffraction peaks exclusively associated with the monoclinic phase of CuO, indicating the formation of a crystalline CuO structure without the presence of other crystalline phases such as Cu_2O. Distinct ZnO diffraction peaks were clearly observed in the **10 $ZnO–CuO–Al_2O_3$** and **Commercial**. In contrast, no detectable ZnO peaks were found in the **1 $ZnO–CuO–Al_2O_3$** and **ALDZnO–$CuO–Al_2O_3$** samples.

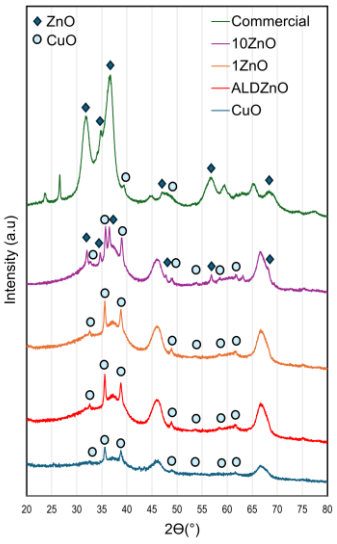

Figure 8: XRD patterns of CZA catalysts

This absence of ZnO peaks could be attributed to one or more of the following reasons: (i) the ZnO peaks may be hidden by the broad diffraction features of the alumina support, making them difficult to resolve; (ii) the ZnO content in the 1 wt% samples may be too low to be distinguished from background noise; or (iii) ZnO may exist in an amorphous state or as highly dispersed and small to be detected in the **1 $ZnO–CuO–Al_2O_3$** and **ALDZnO–$CuO–Al_2O_3$** catalysts.

The crystallite size of CuO in the catalyst was estimated by the Scherrer equation using the peak at 2θ = 35.5° corresponding to the (-111) plane . The crystallite sizes obtained for the CZA catalysts ranged between 24.3 nm and 25.4 nm as summarized in Table 3, suggesting that the second calcination did not significantly the CuO crystallite size in the **1 $ZnO–CuO–Al_2O_3$** and **10 $ZnO–CuO–Al_2O_3$** catalysts.

6.1.2 N_2-Physisorption

CZA catalyst

The nitrogen adsorption–desorption isotherms of the CZA synthesized catalysts (Fig. 9) are all classified as Type IV, characteristic of mesoporous materials with pore diameters between 2 and 50 nm [29]. The key textural parameters obtained from these measurements, including BET surface area, single-point pore volume, and BJH average pore siz, are summarized in Table 3.

Catalyst ID	BET Surface Area [m²/g]	Pore Volume [cm³/g]	Pore Size [nm]	Crystallyte size [nm]
$CuO–Al_2O_3$	92.4	0.31	10.4	24.8
1 $ZnO–CuO–Al_2O_3$	170.8	0.55	10.3	25.4
10 $ZnO–CuO–Al_2O_3$	137.4	0.46	10.3	25.1
ALD$ZnO–CuO–Al_2O_3$	160.6	0.53	10.4	24.3
Commercial	107.1	0.31	10.7	-

Table 3: CZA catalysts textural and crystallographic properties

At high relative pressure ($P/P_0 \approx 0.99$), the total quantity of adsorbed nitrogen follows the trend (Fig 9):

1 ZnO– $CuO–Al_2O_3$ > ALD-$ZnO–CuO–Al_2O_3$ > 10 $ZnO–CuO–Al_2O_3$ > $CuO–Al_2O_3$ ≈ Commercial.

It is noticed that the specific surface area follos the same trend (Table3). This suggests that 1 wt% ZnO sample exhibits the highest accessible pore volume and most accessible surface area among the materials tested, wich is very similar to **ALD-$ZnO–CuO–Al_2O_3$** sample. In contrast, the BJH desorption average pore sizes show only minor variations across all samples (Table 3), indicating that the incorporation of ZnO does not significantly alter the mean pore diameter.

The combined analysis of BET surface area, single-point pore volume, and BJH pore size suggests that the addition of 1 wt% ZnO promotes the formation of a more extensive and accessible mesoporous network. This is supported by the marked increases in both surface area and pore volume, despite a nearly unchanged average pore diameter.

Overall, the catalyst **1 $ZnO–CuO–Al_2O_3$** and **ALD-$ZnO–CuO–Al_2O_3$** display the most favorable textural properties, indicating improved porosity characteristics. Although the **10 $ZnO–CuO–Al_2O_3$** catalyst also shows enhancement relative to the commercial and **$CuO–Al_2O_3$** samples, the results suggest that a low ZnO loading (~1 wt%) is optimal for improving textural features, while higher ZnO contents may reduce these benefits.

One possible explanation for this unusual behavior is that the additional calcination step may have induced structural modifications in the material, although calcination typically tends to reduce porosity. Alternatively, the ZnO itself may contribute mesoporosity to the system. A combination of these effects can not be excluded.

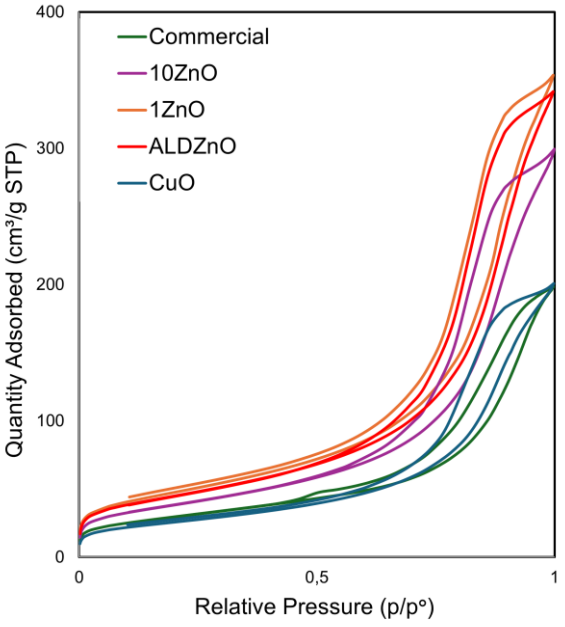

Figure 9: Nitrogen adsorption–desorption isotherms of CZA catalysts.

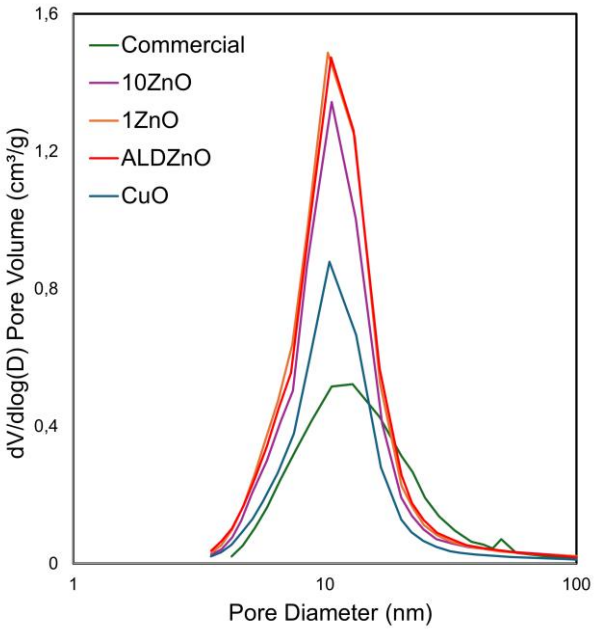

Figure 10: Pore size Distribution of CZA catalysts

ZA catalyst (non copper catalyst)

The nitrogen adsorption–desorption isotherms of the synthesized ZnO–Al_2O_3 reference samples follow the same trend as those of the Cu-based catalysts. Both ALDZnO–Al_2O_3 and 1ZnO–Al_2O_3 exhibit similar surface area and pore volume values. In contrast, the 10ZnO–Al_2O_3 sample shows significantly lower surface area and pore volume (Appendix 1), suggesting that the higher ZnO loading leads to partial pore blockage of the alumina support.

6.1.2. H_2 Temperature-Programmed Reduction (H_2-TPR)

To examine the reducibility of the catalysts, H_2-TPR analysis was carried out, and the corresponding results are presented in Figure11. Two peaks appeared in the range of 180°C to 280 °C suggest that various CuO species are present [30] [31] ,each exhibiting slightly different reducibility characteristics. The reduction peak at low temperature was assigned to the reduction of CuO species that are highly dispersed on the support and the high-temperature reduction peak is associated with the reduction of CuO in its crystalline form[30].

CuO–Al_2O_3, **ALDZnO–CuO–Al_2O_3, 1 ZnO–CuO–Al_2O_3**, and **Commercial** CZA catalyst exhibit two distinct reduction peaks in the temperature range of 180 °C to 280 °C. Unlike the rest of CZA catalysts, **10 ZnO–CuO–Al_2O_3** shows only a single peak within the same range. This behaviour suggest that only one of the two reduction processes occurs. In this case, the observed peak could be attributed to the lower-temperature reduction, suggesting that **10 ZnO-CuO–Al_2O_3** contains the most highly dispersed CuO species.

CuO–Al_2O_3 and **1 ZnO–CuO–Al_2O_3** show similar peak intensity and distribution, with both peaks exhibiting comparable intensities. In contrast, **ALDZnO–CuO–Al_2O_3** shows a higher intensity at the high-temperature peak, altough this peak is still shifted towards lower temperatures compared to the **CuO–Al_2O_3** catalyst. **Commmercial** catalyst exhibit higher intensity peak on the high-reduction peak, suggesting that **Commercial** contains the greater degree of bulk-like CuO species.

Moreover, the synthesized materials could be reduced at temperatures below 275 °C, and the addition of ZnO, especially in the **ALDZnO–CuO–Al_2O_3** and **10 ZnO-CuO–Al_2O_3** samples, improves the reducibility of the copper species at lower temperatures.

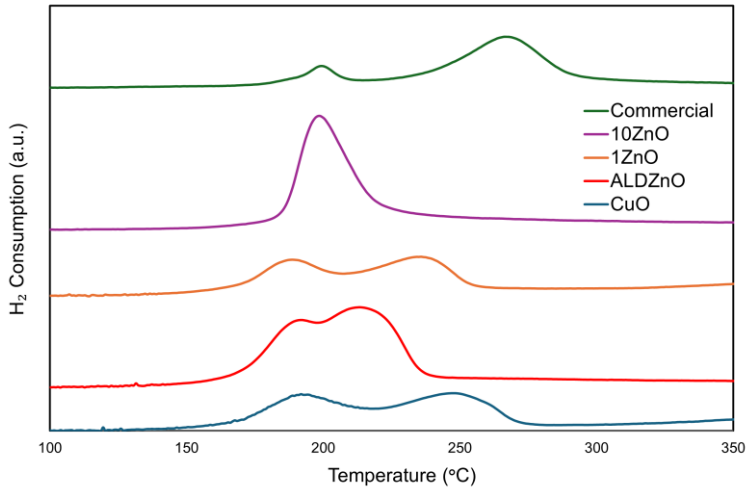

Figure 11: H_2-TPR profile for CZA catalysts

6.2 Catalytic Activity in Methanol Steam Reforming

6.2.1 Methanol Conversion

To determinate the effect of ALD deposition and the amount of ZnO on the performance of the catalyst in the MSR, catalytic test were done for the next CZA catalyst; ; **CuO–Al_2O_3**, **ALDZnO– CuO–Al_2O_3**, **1 ZnO–CuO–Al_2O_3**, **10 ZnO–CuO–Al_2O_3** and **Commercial.** All catalytic activity tests were performed under the same operating conditions, detailed in the Experimental Section, althought Commercial catalyst temperature range was between 200°C and 300°C.

The CZA studied catalyst generally exhibits higher methanol conversion as the reaction temperature increases. However, this trend is disrupted at temperatures above 300 °C for most catalysts. Catalyst deactivation is the most plausible explanation for the resulting decline in catalytic performance.

The CZA catalysts exhibit distinct methanol conversion behaviors depending on the temperature. **ALD ZnO–CuO–Al_2O_3** shows high activity at moderate temperatures, particularly between 250 °C and 325 °C, while **1 ZnO–CuO–Al_2O_3** achieves its highest conversions at higher temperatures, notably in 350 °C. Among all the samples, **10 ZnO–CuO–Al_2O_3** displays the most efficient performance across the temperature range. In contrast, both the **Commercial** and **CuO–Al_2O_3** catalysts exhibit lower methanol conversions, although the limited temperature range tested for the commercial catalyst (up to 300 °C) may have constrained its observed activity.

ALD ZnO–CuO–Al_2O_3 , **1 ZnO–CuO–Al_2O_3** and **10 ZnO–CuO–Al_2O_3** exhibit a better catalytic performance than **Commercial** and **CuO–Al_2O_3**. The results suggest that a low ZnO loading (<10 wt%) is optimal for improving methanol conversion in MSR. Although, 1 **ZnO–CuO–Al_2O_3** and **10 ZnO–CuO–Al_2O_3** reached higher methanol conversion at high temperatures, **ALD ZnO–CuO–Al_2O_3** appears to be the best option below 275 °C and and its stable methanol conversion over a range of temperatures draws attention to its potential.

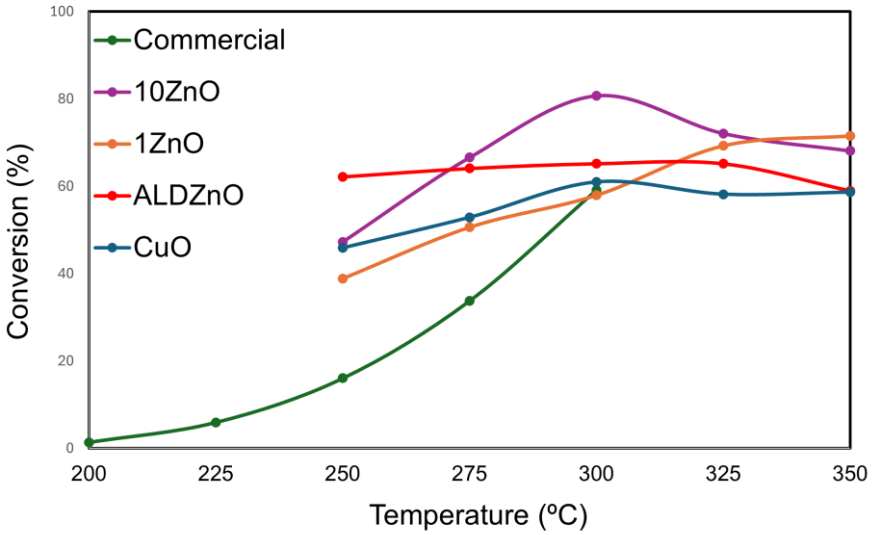

Figure 12: CZA methanol conversion.

6.2.2 Selectivity to CO

To evaluate the effect of ALD deposition and the amount of ZnO on the selectivity towards carbon monoxide during methanol steam reforming (MSR), the same series of CZA catalysts were tested than at 6.2.1 section.

CO selectivity increases with temperature across all studied catalysts, remaining minimal at lower temperatures and becoming more pronounced above 300 °C. The **Commercial** catalyst consistently shows the lowest CO selectivity, although it was not tested beyond 300 °C, where CO formation could potentially rise. Among the ZnO-modified catalysts, **10 ZnO–CuO–Al_2O_3** generally exhibits the highest CO selectivity above all CZA catalysts. At lower temperatures, **ALDZnO–CuO–Al_2O_3** and **CuO–Al_2O_3** display comparatively lower CO selectivity than **1 ZnO–CuO–Al_2O_3** and **10 ZnO–CuO–Al_2O_3**, but this trend shifts at temperatures above 300 °C, where 1 **ZnO–CuO–Al_2O_3** shows reduced CO formation relative to **ALDZnO–CuO–Al_2O_3** and **CuO–Al_2O_3**.

The results suggest that a 1 wt% ZnO loading is optimal for avoiding higher CO selectivity at temperatures above 300 °C. However, the CO production at high temperatures might still not be low enough to be considered a definitive solution. ALD deposition appears as a fitting technique in order to decrease the CO production on temperatures in the range of 250°C to 275 °C. **Commercial** low CO selectivity demonstrates that there is still room for improvement in the optimization of the synthesized catalyst.

Finding a compromise between high methanol conversion and low CO selectivity is a main goal of Methanol Steam Reforming. **ALD ZnO–CuO–Al_2O_3** performance at 275 °C reveals high methanol conversions and low CO selectivity, inducing **ALD ZnO–CuO–Al_2O_3** as a suitable candidate for MSR.

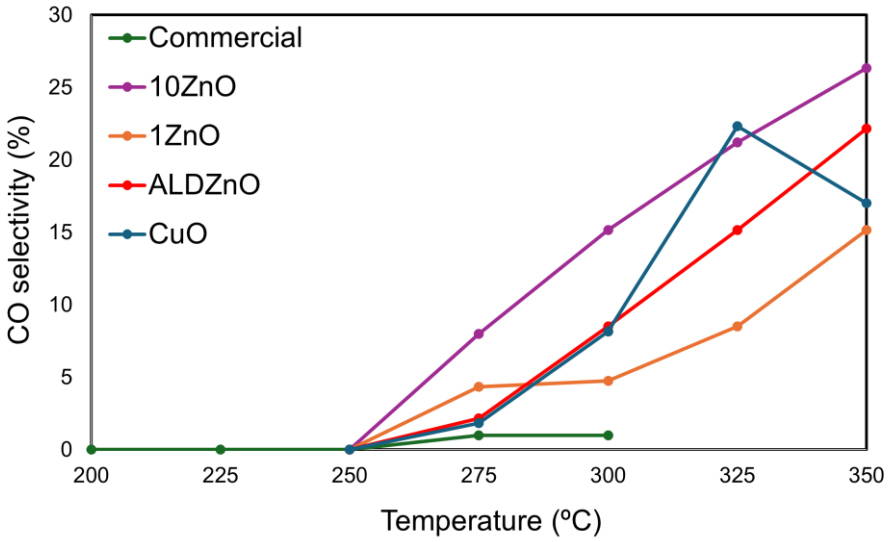

Figure 13:CZA CO selectivity

6.2.3 Correlation Between Physicochemical Properties and Catalytic Performance

All synthesized catalysts exhibit a well-defined crystalline CuO structure, while all of them show catalytic activity as evidenced by the methanol conversion values. The CuO structure emerges as a key factor in ensuring good catalytic performance. The effect of the presence of hexagonal wurtzite ZnO structure on the catalytic performance is not clear, as both **10 ZnO–CuO–Al_2O_3** and the **Commercial** catalyst contain it, yet they differ in methanol conversion and CO selectivity values.

Catalysts with the most favorable textural properties do not always result in better methanol conversions. This might be explained by a higher degree of metal dispersion/effective distribution of active sites, which can be compatible with a lower surface area. For better understanding, the dispersion of active sites (commonly Cu sites) can be estimated using characterization techniques such as N_2O chemisorption or transmission electron microscopy (TEM), among others.

Synthesized catalysts exhibit reduction peaks below 300 °C, allowing the reduction to Cu^0 at relatively low temperatures, and providing the maximum number of active catalytic sites. The coexistence of dispersed CuO with crystalline CuO may provide benefits in enhancing catalytic activity.

10. CONCLUSIONS

This study focused on optimizing and minimizing the amount of ZnO catalytic performance of $CuO/ZnO/Al_2O_3$ (CZA) catalysts for methanol steam reforming (MSR) by exploring different ZnO loadings and synthesis techniques, including conventional wet impregnation and Atomic Layer Deposition (ALD).

All synthesized catalysts exhibited a well-defined monoclinic CuO crystalline phase. While the presence of hexagonal wurtzite ZnO was confirmed in catalysts with higher ZnO content (10 wt%) and the commercial sample, its direct impact on catalytic performance remains inconclusive.

Textural characterization revealed that catalysts with 1 wt% ZnO loading exhibited superior properties, such as higher surface area, larger pore volume, and enhanced pore accessibility, compared to those with higher ZnO content or no ZnO. However, these improved textural features did not always result in better methanol conversions. The catalyst with 10 wt% ZnO showed the highest methanol conversion despite not possessing the best textural characteristics. A plausible explanation for the improved catalytic performance might be a higher degree of metal dispersion and a more effective distribution of active sites.

H_2-TPR analysis demonstrated reduction peaks below 300 °C for all catalysts, suggesting facile reduction to metallic Cu^0 and thus a high availability of active sites. Catalysts exhibited two distinct CuO species, dispersed and bulk-like, that may synergistically enhance catalytic activity.

Catalytic testing showed that methanol conversion generally increased with temperature up to around 300 °C, beyond which a decrease in activity was observed, possibly indicating the onset of catalyst deactivation. Among the synthesized catalysts, **10 ZnO–CuO–Al_2O_3** achieved the highest conversion (80% at 300 °C). ALD-synthesized catalysts demonstrated stable performance at lower temperatures, with lower CO selectivity, highlighting the potential of ALD techniques for optimizing catalyst properties.

The commercial catalyst displayed the lowest CO selectivity values, emphasizing the need to improve synthesized catalysts to be better than **Commercial** catalyst. ALD deposition proved effective in reducing CO formation in the 250–275 °C range.

In summary, this work underscores the complex interplay between catalyst composition, synthesis method, and physicochemical properties in determining MSR performance. The ALD technique offers promising avenues for further catalyst optimization to achieve better balance between activity and selectivity.

11. REFERENCES AND NOTES

(1) Zhang, M.; Liu, D.; Wang, Y.; Zhao, L.; Xu, G.; Yu, Y.; He, H. Recent Advances in Methanol Steam Reforming Catalysts for Hydrogen Production. *Catalysts*. Multidisciplinary Digital Publishing Institute (MDPI) January 1, 2025. https://doi.org/10.3390/catal15010036.

(2) Feng, W.; Ji, P.; Chen, B.; Zheng, D. Analysis of Methanol Production from Biomass Gasification. *Chem Eng Technol* **2011**, *34* (2), 307–317. https://doi.org/10.1002/ceat.201000346.

(3) Azhari, N. J.; Erika, D.; Mardiana, S.; Ilmi, T.; Gunawan, M. L.; Makertihartha, I. G. B. N.; Kadja, G. T. M. Methanol Synthesis from CO2: A Mechanistic Overview. *Results in Engineering* **2022**, *16*. https://doi.org/10.1016/j.rineng.2022.100711.

(4) Hadi, M.; Alavi, S. M.; Rezaei, M.; Akbari, E.; Tabarkhoon, F. Methanol Steam Reforming over CuO/MgAl2O4 Nanocatalysts: Influence of Copper Oxide Loading and Process Parameters on Hydrogen Production. *Fuel* **2025**, *399*. https://doi.org/10.1016/j.fuel.2025.135678.

(5) Araya, S. S.; Liso, V.; Cui, X.; Li, N.; Zhu, J.; Sahlin, S. L.; Jensen, S. H.; Nielsen, M. P.; Kær, S. K. A Review of the Methanol Economy: The Fuel Cell Route. *Energies (Basel)* **2020**, *13* (3). https://doi.org/10.3390/en13030596.

(6) Yadav, D.; Lu, X.; Vishwakarma, C. B.; Jing, D. Advancements in Microreactor Technology for Hydrogen Production via Steam Reforming: A Comprehensive Review of Experimental Studies. *Journal of Power Sources*. Elsevier B.V. November 30, 2023. https://doi.org/10.1016/j.jpowsour.2023.233621.

(7) Shishido, T.; Yamamoto, Y.; Morioka, H.; Takaki, K.; Takehira, K. Active Cu/ZnO and Cu/ZnO/Al2O3 Catalysts Prepared by Homogeneous Precipitation Method in Steam Reforming of Methanol. *Appl Catal A Gen* **2004**, *263* (2), 249–253. https://doi.org/10.1016/j.apcata.2003.12.018.

(8) Guo, J.; Cui, H.; Zhang, H.; Du, J. Integrated System Utilizing Methanol Steam Reforming Process for Hydrogen Production Combined with Methane-Hydrogen Gas Turbine Multi-Cascade Generation. *Appl Therm Eng* **2025**, *271*. https://doi.org/10.1016/j.applthermaleng.2025.126324.

(9) Wang, G.; Wang, F.; Chen, B. Performance Study on Methanol Steam Reforming Rib Micro-Reactor Withwaste Heat Recovery. *Energies (Basel)* **2020**, *13* (7). https://doi.org/10.3390/en13071564.

(10) Yu, K. M. K.; Tong, W.; West, A.; Cheung, K.; Li, T.; Smith, G.; Guo, Y.; Tsang, S. C. E. Non-Syngas Direct Steam Reforming of Methanol to Hydrogen and Carbon Dioxide at Low Temperature. *Nat Commun* **2012**, *3*. https://doi.org/10.1038/ncomms2242.

(11) Neto, R. M.; Lenzi, G. G.; Pimenta, J. L. C. W.; Fornari, A. C.; Dos Santos, O. A. A.; De Matos Jorge, L. M. Analysis of Carbon Monoxide Production in Methanol Steam Reforming Reactor for Generating Hydrogen. *Acta Scientiarum - Technology* **2019**, *41* (1). https://doi.org/10.4025/actascitechnol.v41i1.39926.

(12) Sá, S.; Sousa, J. M.; Mendes, A. Steam Reforming of Methanol over a CuO/ZnO/Al2O3 Catalyst, Part I: Kinetic Modelling. *Chem Eng Sci* **2011**, *66* (20), 4913–4921. https://doi.org/10.1016/j.ces.2011.06.063.

(13) Shi, Z.; Peng, Q.; Wang, H.; Huang, Z.; Liu, H.; Tian, X.; Yan, F.; Yin, R. Catalyst, Reactor, Reaction Mechanism and CO Remove Technology in Methanol Steam Reforming for Hydrogen Production: A Review. *Fuel Processing Technology*. Elsevier B.V. December 15, 2023. https://doi.org/10.1016/j.fuproc.2023.108000.

(14) Li, Y.; Luo, C.; Su, Q. Performance of Cu/ZnO/Al2O3 Catalysts Prepared by Sol–Gel Methods on Methanol Steam Reforming. *Energies (Basel)* **2023**, *16* (23). https://doi.org/10.3390/en16237803.

(15) Ajamein, H.; Haghighi, M.; Minaei, S.; Alaei, S. Texture/Phase Evolution during Microwave Fabrication of Nanocrystalline Multicomponent (Cu/Zn/Al)O Metal Oxides with Varying Diethylene Glycol Content Applied in Hydrogen Production. *Int J Hydrogen Energy* **2018**, *43* (51), 22838–22851. https://doi.org/10.1016/j.ijhydene.2018.10.174.

(16) Borgohain, P.; Tiwari, P.; Upadhyay, R. K. Optimization of Cu/Zn/Al2O3 and Cu-Ga/Zn/Al2O3 Catalysts Using Response Surface Methodology for Methanol Steam Reforming for Hydrogen Production. *Journal of the Energy Institute* **2025**, *121*. https://doi.org/10.1016/j.joei.2025.102155.

(17) Huang, Z.; Guo, C.; Guo, W.; Zhang, Y.; Huang, S.; Qin, H.; Xie, W.; Gao, P.; Xiao, H. Gallium-Induced Structural Modification over Gel-Derived CuZnGaAlOx Catalysts for Methanol Steam Reforming. *Ceram Int* **2025**. https://doi.org/10.1016/j.ceramint.2025.02.058.

(18) Murcia-Mascarós, S.; Navarro, R. M.; Gómez-Sainero, L.; Costantino, U.; Nocchetti, M.; Fierro, J. L. G. Oxidative Methanol Reforming Reactions on CuZnAl Catalysts Derived from Hydrotalcite-like Precursors. *J Catal* **2001**, *198* (2), 338–347. https://doi.org/10.1006/jcat.2000.3140.

(19) Yaakob, Z.; Adib Ibrahim, M.; Ramli Wan Daud, W. *Multi-Composition Cu-Zn-Al Catalyst Supported on ZSM-5 for Hydrogen Production*; 2009. https://www.researchgate.net/publication/242240029.

(20) Li, Y.; Ma, Z. yu; Qi, Z. yan; Xue, Z. an; Zhou, X. long; Guo, H. Investigation of Methanol Steam Reforming Reactors with Different Catalyst Support Structures on Hydrogen Production Efficiency and Methanol Conversion. *Fuel* **2025**, *393*. https://doi.org/10.1016/j.fuel.2025.135079.

(21) Li, D.; Xu, F.; Tang, X.; Dai, S.; Pu, T.; Liu, X.; Tian, P.; Xuan, F.; Xu, Z.; Wachs, I. E.; Zhu, M. Induced Activation of the Commercial Cu/ZnO/Al2O3 Catalyst for the Steam Reforming of Methanol. *Nat Catal* **2022**, *5* (2), 99–108. https://doi.org/10.1038/s41929-021-00729-4.

(22) Kamsuwan, T.; Guntida, A.; Praserthdam, P.; Jongsomjit, B. Differences in Deterioration Behaviors of Cu/ZnO/Al2O3Catalysts with Different Cu Contents toward Hydrogenation of CO and CO2. *ACS Omega* **2022**, *7* (29), 25783–25797. https://doi.org/10.1021/acsomega.2c03068.

(23) Onn, T. M.; Küngas, R.; Fornasiero, P.; Huang, K.; Gorte, R. J. Atomic Layer Deposition on Porous Materials: Problems with Conventional Approaches to Catalyst and Fuel Cell Electrode Preparation. *Inorganics*. MDPI Multidisciplinary Digital Publishing Institute March 1, 2018. https://doi.org/10.3390/inorganics6010034.

(24) Jung, M. J.; Kim, D.; Kim, H. C.; Kim, S.; Kim, Y.; Kwon, S. H.; Lee, W. J. ZnO Thin Films with Stable, Tunable Electrical and Optical Properties Deposited by Atomic Layer Deposition Using Et2Zn:NEtMe2 Precursor. *Appl Surf Sci* **2025**, *682*. https://doi.org/10.1016/j.apsusc.2024.161728.

(25) Johnston, L.; Obenlüneschloß, J.; Khan Niazi, M. F.; Weber, M.; Lausecker, C.; Rapenne, L.; Roussel, H.; Sanchez-Velazquez, C.; Bellet, D.; Devi, A.; Muñoz-Rojas, D. Assessing the Potential of Non-Pyrophoric Zn(DMP) 2 for the Fast Deposition of ZnO Functional Coatings by Spatial Atomic Layer Deposition . *RSC Applied Interfaces* **2024**. https://doi.org/10.1039/d4lf00160e.

(26) Rowlette, P. C.; Allen, C. G.; Bromley, O. B.; Dubetz, A. E.; Wolden, C. A. Plasma-Enhanced Atomic Layer Deposition of Semiconductor Grade ZnO Using Dimethyl Zinc. *Chemical Vapor Deposition* **2009**, *15* (1–3), 15–20. https://doi.org/10.1002/cvde.200806725.

(27) Sinha, S.; Sarkar, S. K. ZnO as Transparent Conducting Oxide by Atomic Layer Deposition. In *2013 IEEE 39th Photovoltaic Specialists Conference (PVSC)*; 2013; pp 1183–1186. https://doi.org/10.1109/PVSC.2013.6744351.

(28) Greenberg, B. L.; Anderson, K. P.; Jacobs, A. G.; Cendejas, A. J.; Hajzus, J. R.; Patterson, E. A.; Wollmershauser, J. A.; Feigelson, B. N. Conformal Coating of Macroscopic Nanoparticle Compacts with ZnO via Atomic Layer Deposition. *Journal of Vacuum Science & Technology A* **2024**, *42* (1). https://doi.org/10.1116/6.0003182.

(29) *INTERNATIONAL UNION OF PURE AND APPLIED CHEMISTRY PHYSICAL CHEMISTRY DIVISION COMMISSION ON COLLOID AND SURFACE CHEMISTRY INCLUDING CATALYSIS* REPORTING PHYSISORPTION DATA FOR GAS/SOLID SYSTEMS with Special Reference to the Determination of Surface Area and Porosity Reporting Physisorption Data for Gas/Solid Systems-with Special Reference to the Determination of Surface Area and Porosity*; 1985.

(30) Liu, H.; Zhu, W.; Zhou, X.; Wei, B.; Bing, L.; Han, D.; Wang, G.; Wang, F. Fabrication of Cu-Based Catalysts for the Synthesis of Neopentyl Glycol from Hydroxypivalaldehyde Hydrogenation: Studies on the Role of Zr Promoter. *Reaction Kinetics, Mechanisms and Catalysis* **2024**. https://doi.org/10.1007/s11144-024-02768-x.

(31) Mohamed, A. T.; Ahmad, Y. H.; Anwer, A. H.; Soliman, A.; Saad, M. A. H.; Aroua, M. K.; Al-Qaradawi, S. Y.; Benamor, A. CO2 Conversion to Dimethyl Ether on Cu/ZnO/Al2O3-ZSM-5 Tandem Catalysts in a Double-Bed Reactor: Tuning the ZSM-5 Catalyst Acidity and Porosity. *Energy and Fuels* **2025**, *39* (4), 2059–2074. https://doi.org/10.1021/acs.energyfuels.4c04512.

12. ACRONYMS

MSR: Methanol Steam Reforming

IREC: Institut de Recerca en Energia de Catalunya

CZA: $CuO/ZnO/Al_2O_3$

ALD: Atomic Layer Deposition

SOFCs: solid oxide fuel cells

DEZ: diethylzinc

DMZ: dimethylzinc

DEZMEA: diethylzinc-dimethylethylamine

XRD: X-ray crystallography

H_2-TPR: Hydrogen temperature-programmed reduction

.

APPENDICES

APPENDIX 1: N_2-PHYSISORPTION ZA GRAPHS AND TABLES

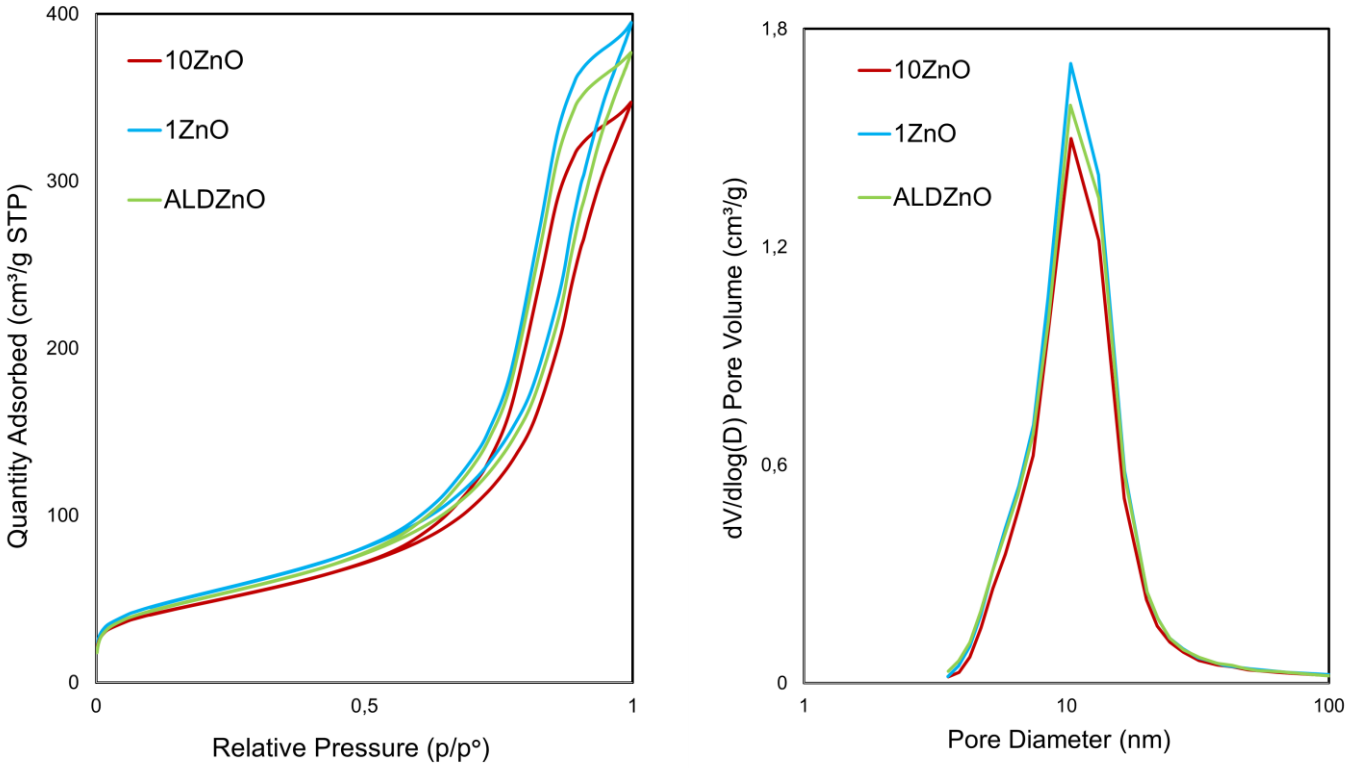

Catalyst ID	BET Surface Area [m^2/g]	Pore Volume [cm^3/g]	Pore Size [nm]
ALDZnO–Al_2O_3	183.4	0.6	10.22
1ZnO–Al_2O_3	193.2	0.6	10.32
10ZnO–Al_2O_3	170.9	0.5	10.37

Table 4: ZA references textural properties